SUPPLEMENTARY MATERIAL to

Characterization of non-symbiotic tomato hemoglobin

Ioanitescu, Iulia, Dewilde, Sylvia, Kiger, Laurent, Marden, Michael C., Moens, Luc, Van Doorslaer, Sabine

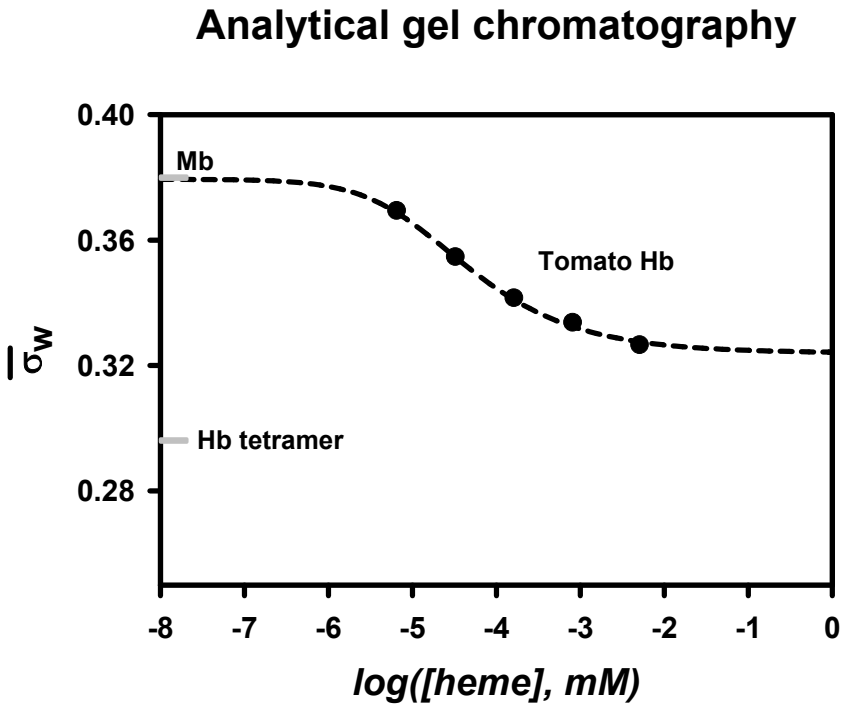

Figure A1*:* Analytical gel chromatography of SOLly GLB1. Weight-averaged partition coefficients ($\overline{\sigma}_w$) as a function of protein concentration (mM in heme). The simulation represents the best fit for the equilibrium constant and end points (0.38 and 0.32). Horse heart Mb (monomer) and Hb A (tetramer) were used as references (in gray).

pH dependence of the absorption spectra of deoxy ferrous SOLly GLB1

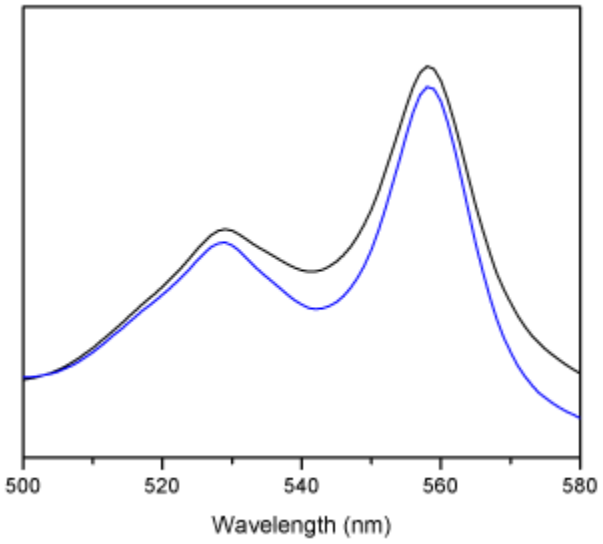

Figure U1. Comparison between the absorption spectra (500-580 nm) of deoxy ferrous SOLly at pH 7 (blue) and pH 8.5 (black). GLB1. We observe a broadening and increase of the peak around 560 nm, corresponding to an increase in the contribution of a HS ferrous (typical absorbance maxima at 432 and 560 nm (30)

RESONANCE RAMAN: comparison between SOLly GLB1 at pH 7 and pH 8.5.

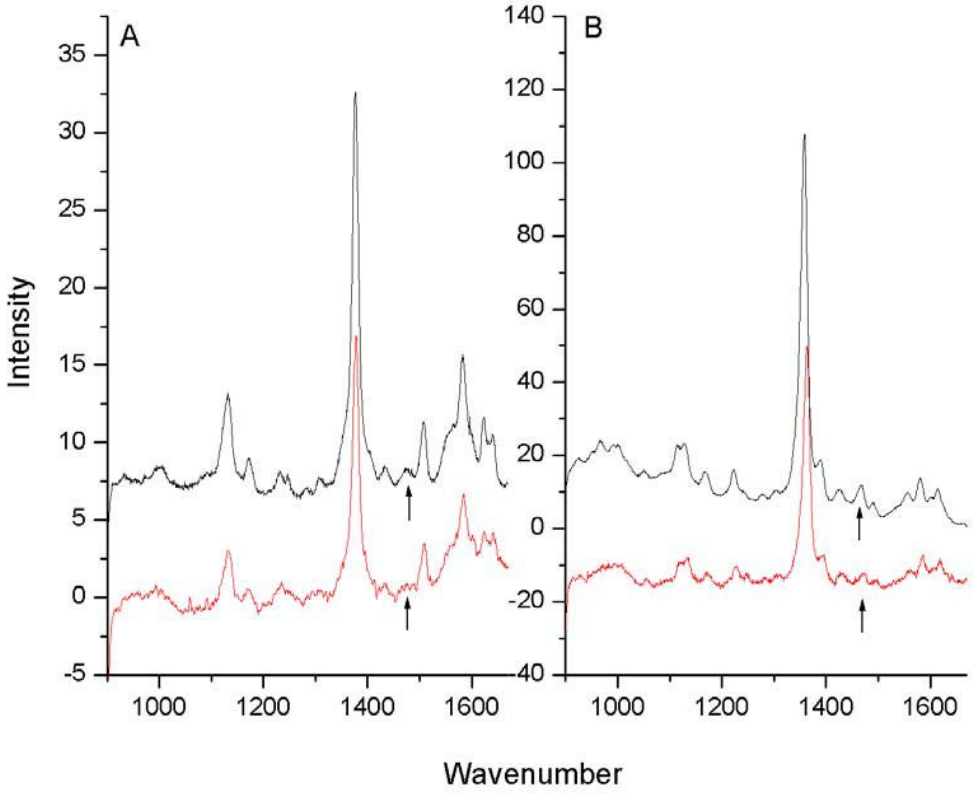

Figure R1. Comparison between resonance Raman spectra of tomato SOLly GLB1 in the ferric (A) and deoxy ferrous (B) form at pH 8.5 (black) and pH 7 (red). The arrows show the position of the ν_3 of the aquomet form (A) and the contribution of the pentacoordinated ferrous form (B). In both cases there is a decrease of the signal upon lowering of the pH.

RESONANCE RAMAN: DERIVATION OF CORE SIZE

According to reference (32), the core-size can be computed using formula

$$\nu = K(A-d) \qquad \text{(S1)}$$

with K, A from ref. 32 and d= C_t-N distance (porphyrin-center to pyrrole nitrogen).

Table S1 shows the distances *d* derived for the ferric form of Soly GLB1. The last row shows the average of the distances.

Table S1

			Ferric SOLly GLB1	
	K (cm^{-1} $Å^{-1}$)	*A* (Å)	*RR positon* (cm^{-1})	*d*(C_t-N) (Å)
ν_{10}	517.2	5.16	1636	1.9968
ν_{38}	551.7	4.80	1550	1.9905
ν_3	448.3	5.35	1502	1.9996
ν_2	390.8	6.03	1578	1.9921
				1.9948

THEORY OF PULSED EPR EXPERIMENTS

In case of a bis-histidine coordination of the ferric heme group, as observed for SOLly GLB1, the Fe(III) is in a low-spin state (S=1/2). The unpaired electron can interact with nuclei with nuclear spins I>0 in its environment. Generally such spin systems are described by a spin Hamiltonian. The spin Hamiltonian of an S=1/2, I=1 system (e.g. Fe(III) – ^{14}N) can be described in terms of the **g** matrix, the hyperfine matrix **A**, the nuclear Zeeman interaction and the nuclear-quadrupole tensor **P** and is given by the relation:

$$H = \frac{\beta_e}{h} B_0 gS + SAI - \frac{\beta_n}{h} B_0 g_n I + IPI \qquad \text{(S2)}$$

where the first term is the electron Zeeman interaction, the second one describes the hyperfine interaction between the unpaired electron, and the nuclear spin, the third one is the nuclear Zeeman contribution and the last term reflects the nuclear-quadrupole interaction (11).

The HYSCORE spectra of such an *S*=1/2, *I*=1 system is dominated by the cross-peaks between the double-quantum (DQ) frequencies (Dikanov, S.A., Yu.D. Tsvetkov, M.K. Bowman and A.V. Astashkin. 1982. Parameters of quadrupole coupling of ^{14}N nuclei in chlorophyll a cations determined by the electron spin echo method**.** Chem. Phys. Lett. 90, 149-153; Dikanov, S.A., L. Xun, A.B. Karpiel, A.M. Tyryshkin, and M.K. Bowman. 1996. Orientationally-Selected Two-Dimensional ESEEM Spectroscopy of the Rieske-Type Iron-Sulfur Cluster in 2,4,5-Trichlorophenoxyacetate Monooxygenase from *Burkholderia cepacia* AC1100. J. Am. Chem. Soc. 118, 8408-8416)

$$\nu_{DQ}^{\alpha,\beta} = 2\sqrt{\left(\frac{a}{2} \pm \nu_I\right)^2 + K^2\left(3+\eta^2\right)} \qquad \text{(S3)}$$

where a is the hyperfine coupling at a particular observer position and the nuclear Zeeman frequency $\nu_I = -g_n\beta_n B_0 / h$. From the position of the DQ cross-peaks and using the above equation, a first idea about the magnitude of the hyperfine interaction and of $K^2(3+\eta^2)$ can be obtained, which can then be optimised by simulating the spectra.

For an *S*=1/2, *I*=1/2 system (e.g. Fe(III) – ^{1}H), the basic nuclear transition frequencies in the two m_S manifolds are given by

$$\nu^{\alpha,\beta} = \sqrt{\left(\frac{A}{2} \pm \nu_I\right)^2 + (B/2)^2} \qquad \text{(S4)}$$

A and B describe the secular and pseudosecular part of the hyperfine coupling (11). In the HYSCORE spectra experiment, the correlation between the nuclear transitions lead to cross-peaks between the basic frequencies as outlined in detail in ref. 11. Since B is related to the dipolar coupling which in turn depends on the distance between the unpaired electron and the

proton, both proton HYSCORE and CP experiments can reveal important information on the Fe-H distance (11), as is extensively used in this work.

PULSED EPR ANALYSIS

The following analysis of the pulsed-EPR data is fully based on the strategy that we outlined earlier for the study of ferric heme complexes (16)

a) First step in the analysis.

Based on the earlier isotope-labeling experiments on FePPIX(im)$_2$, the double-quantum (DQ) cross-peaks of the porphyrin and histidine nitrogens could be identified (15). In a first step, the hyperfine and nuclear-quadrupole interactions of the porphyrin nitrogens are simulated (simulation parameters, see Table II). Within the experimental error, the four heme nitrogens are equivalent. The below figure S1 shows the simulations (red) of the heme ^{14}N contributions together with the experimental spectra (blue) for different observer positions (magnetic field settings).

At the last observer position ($g = g_x$), only one set of cross-peaks between DQ frequencies could be observed in the HYSCORE spectra (Figure S1d). However, the spin echo at this position was very low, so that several signals may have been lost in the noise. Since for FeTPP(4-MeIm)$_2$ (16) and for FePPIX(Im)$_2$ (15) two DQ sets were observed (one of the heme nitrogens, the other from the histidine nitrogens), 3-pulse ESEEM experiments were performed, which revealed indeed the existence of two sets (Figure S2).

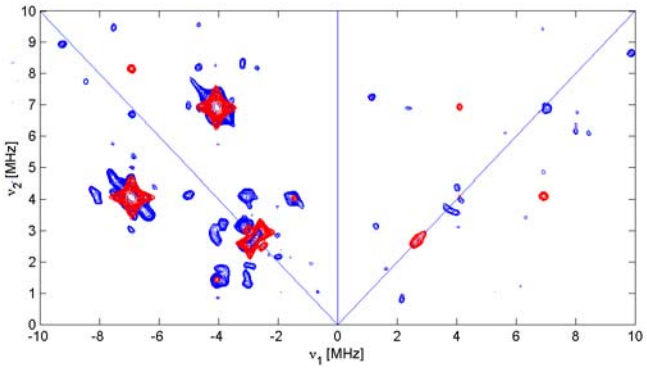

Figure S1 (a): $g=g_z$; simulation of contribution of porphyrin nitrogens

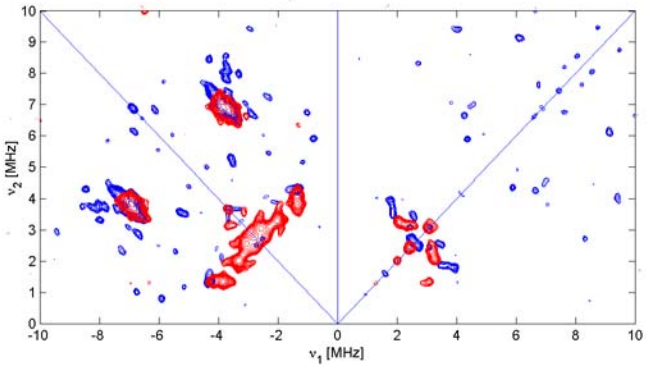

Figure S1 (b): g=2.055; simulation of contribution of porphyrin nitrogens

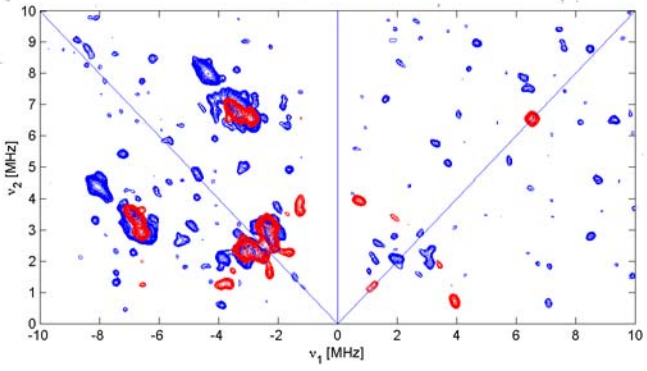

Figure S1 (c): $g=g_y$; simulation of contribution of porphyrin nitrogens

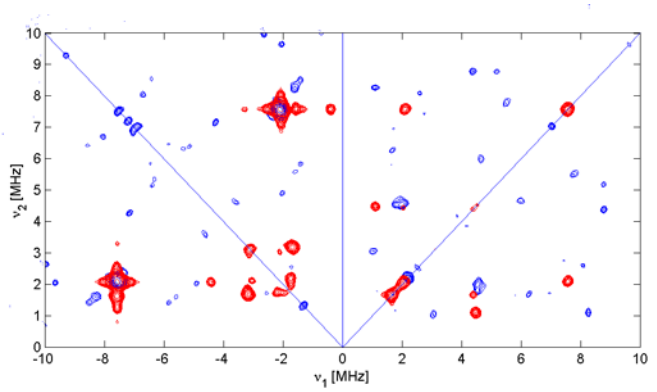

Figure S1 (d): $g=g_x$; simulation of contribution of porphyrin nitrogens

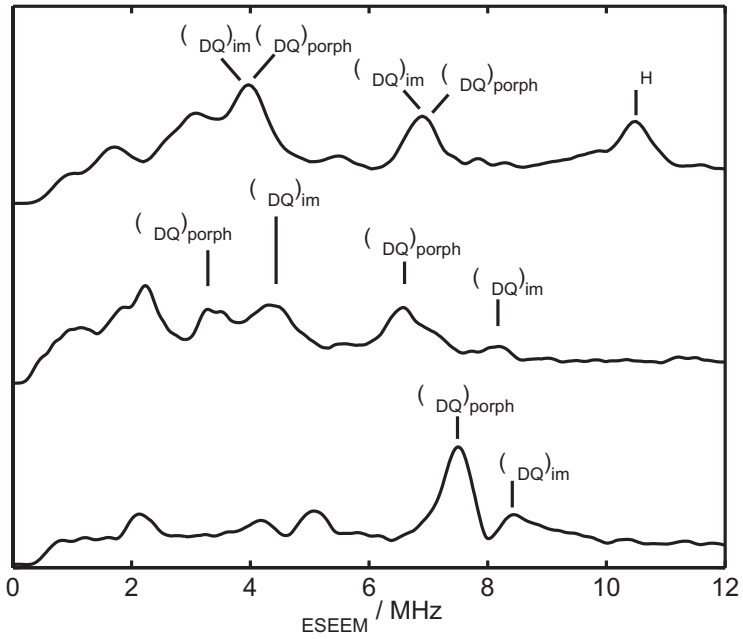

Figure S2: 3-pulse ESEEM spectra at observer position, g= g_z (top), g=g_y (middle), g = g_x (bottom). Note that in the bottom spectrum, two sets of ν^{α}_{DQ} frequencies could be resolved.

MAJOR RESULT of first step: From the simulation parameters in Table II and using the knowledge that (i) the largest nuclear-quadrupole of the heme nitrogens is in the heme plane, perpendicular to the Fe-N_{heme} bond and (ii) $\boldsymbol{g_z}$ || the heme normal, the g axes can be oriented in the molecular frame : $\mathbf{g_x}(\mathbf{g_y})$ is tilted 10^{o} ($\pm 10^{o}$) away from N_{heme}-Fe-N_{heme}.

b) second step in the analysis.

In this step we concentrate on the interactions with the nearest protons. In this case, we focus on the interactions with the nearest histidine protons (indicated as NP). For this, we performed combination-peak experiments (Figure S3) together with proton HYSCORE

experiments (Figure S4). In the CP spectra, interactions of the electron spin and the 4 nitrogens of the porphyrin ring give rise to the lines between 1 and 8 MHz (Figure S3). The proton peaks of interest are seen in the 20-25 MHz region. They are the "proton sum combination peaks", i.e. peaks found at positions that are the summation of the basic frequencies. If we consider the spectrum in Figure S3a, we see two peaks in this region. The position of the first peak coincides with twice the proton Larmor frequency, $2\nu_H$ (= 20.86 MHz for this chosen field). The absence of a detectable shift of this line from $2\nu_H$ allows us to conclude that this peak is caused by interactions of the unpaired electron of Fe^{III} with distant protons, those which are separated from the electron spin by a distance greater than 5 Å. The other peak is caused by the interaction of Fe^{III} with the four nearest protons of the imidazole ring (NP). The shift of this peak from $2\nu_I$ ($\Delta = \nu_+ - 2\nu_H$) is depending on the strength of the magnetic field, $\boldsymbol{B}_0$. As we showed earlier (16), we can use the shift of the NP combination peak with respect to the double nuclear-Zeeman frequency ((14), Figure S3) in combination with the proton HYSCORE spectra (Figure S4) to determine information on the $Fe-^1H$ distance (r) and on the orientation of the histidine planes. The latter can be deduced from the orientation of the ($Fe-^1H$) vector, which is determined by the angles θ (the angle between the $\boldsymbol{g}_z$ and the Fe-H axis) and φ (angle between the projection of the Fe-H axis in the ($\boldsymbol{g}_x$, $\boldsymbol{g}_y$) plane and the $\boldsymbol{g}_x$ axis), if the histidine planes are assumed to be approximately parallel with the heme normal (thus perpendicular to the heme plane). In the case of SOLly GLB1, the g values indicate that the histidine planes are not twisted severely, so that this assumption may be considered valid (see main text).

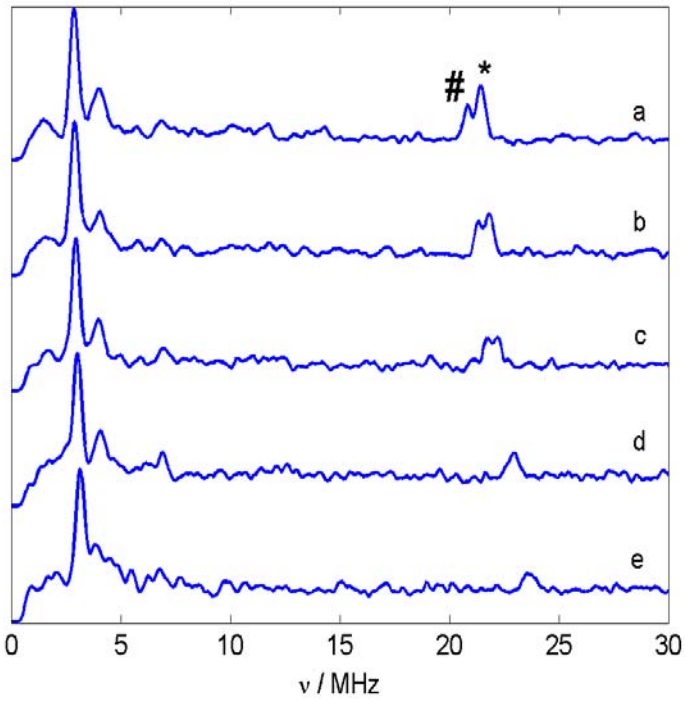

Figure S3: CP experiments, at different g values: 2.84 (a), 2.78 (b), 2.73 (c), 2.62 (d) and 2.53 (e).

# indicates $2\nu_H$ and * indicates ν_+ of nearest protons.

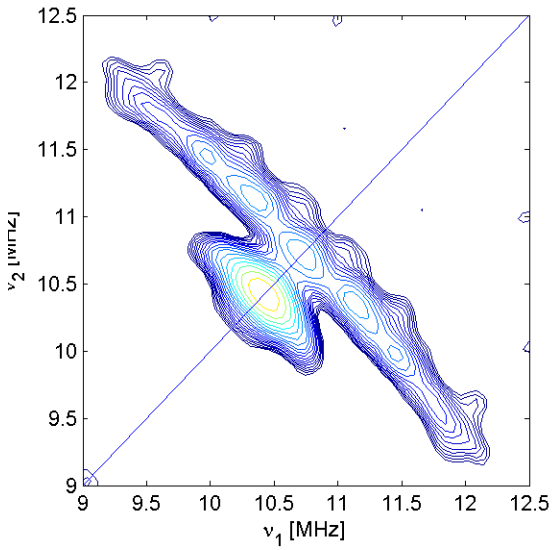

Figure S4: Example of a matched proton. HYSCORE spectrum at $g=g_z$

Figure S5 shows different sets of simulations whereby the influence of the variation of φ is tested. a_{iso}, the isotropic part of the hyperfine interaction, is negative and small in accordance with earlier findings (14). From Figure S5 it can be seen that the solutions with φ = 30-55^{o} lie within the experimental error. Note that, due to the nature of EPR experiments, the sign of φ cannot be determined.

Figure S5: different simulations, whereby the value of φ is varied. Left: prediction of the expected shifts of the CP peaks versus the experiment, middle: experiment (blue) + simulation (red) of proton HYSCORE at $g=g_z$; right: experiment (bleu) + simulation (red) of proton HYSCORE at $g=g_y$.

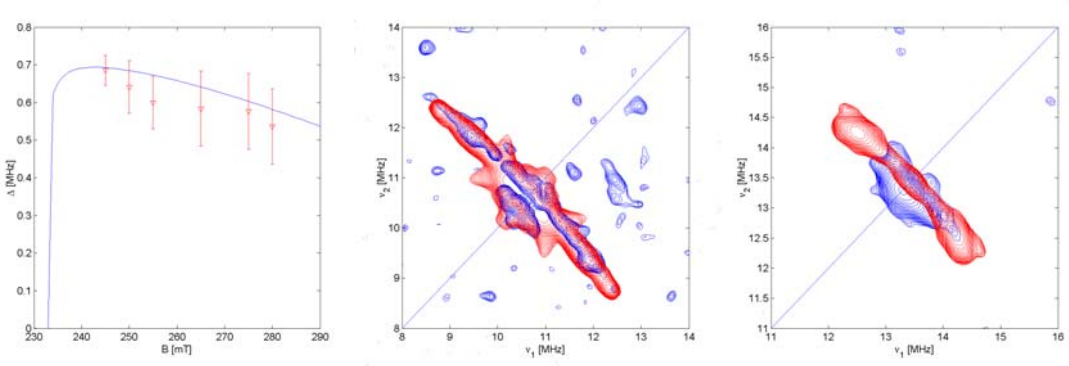

Fit 1: r=0.325 nm, a_{iso} = -0.5 MHz, θ=32^{o}, φ=(±)30^{o} (NOTE: deviation in $g=g_y$)

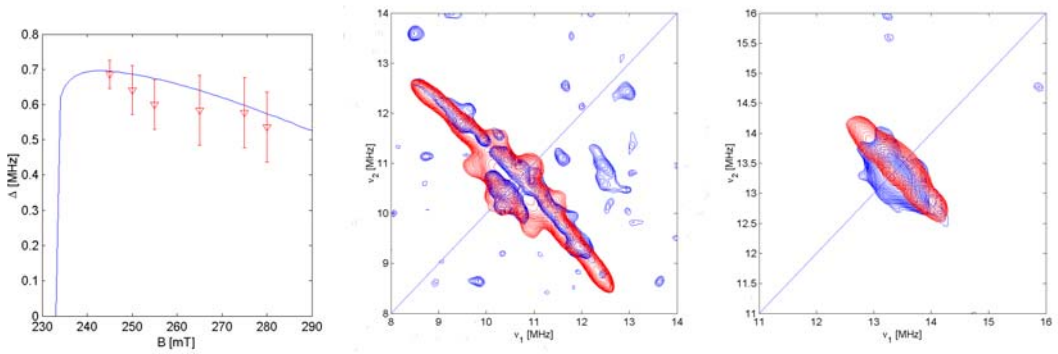

Fit 2: r=0.325 nm, a_{iso} = -0.5 MHz, θ=32^{o}, φ=(±)45^{o}

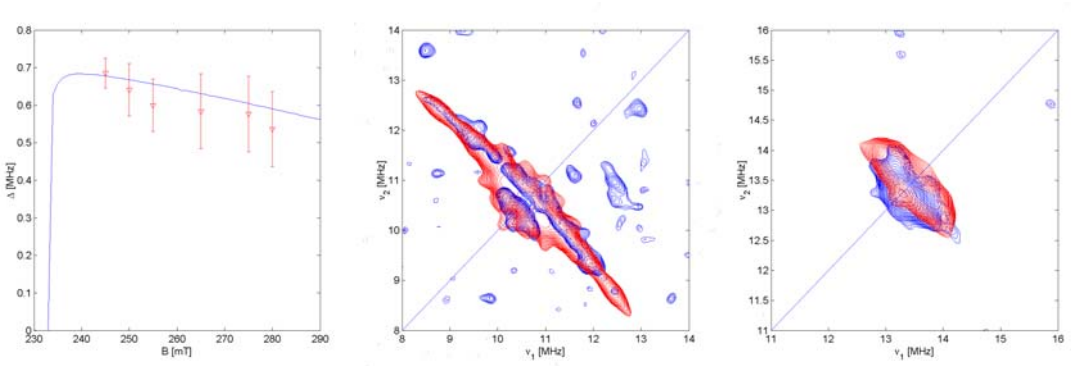

Fit 3: r=0.325 nm, a_{iso} = -0.5 MHz, θ=32^{o}, φ=(±)55^{o} (NOTE: deviation in g=g_z)

We can now combine these results with the counter-rotation principle (46): Based crystal-field considerations one can derive that if the $\boldsymbol{g}_x$ axis deviates over an angle ζ from the N_{heme}-Fe-N_{heme} axis (here: ζ =10^{o} (± 10^{o})), the ligand planes will rotate over an angle ζ_0 in the counterdirection. A simple one-electron treatment gives ζ=-ζ_0, whereas more thorough theoretical derivations show that this is a too strict rule (46). However, one can use the following rule-of-thumb: if –45^{o} < ζ < 0^{o}, ζ_0 will not exceed 45^{o}. In case of two axial histidines with different orientation, only one of the histidines will determine the magnetic axes (46). Comparison with heme proteins with comparable *g* values (e.g. bovine cyt b_5), indicates that for ζ =10^{o} (± 10^{o}), ζ_0 is -15^{o} (± 15^{o}) (46). Note that the above determined parameter φ = |ζ-ζ_0|. Considering that φ was found to be between 30-55^{o}, this seems to indicate that for one of the two histidines, ζ_0 =-20^{o} (± 10^{o}), which is a solution for ζ =10^{o} (± 10^{o})) that is compatible with all above EPR data (Figure S6). For the second histidine, different possibilities can be considered, since the HYSCORE and CP experiments are insensitive to the sign of φ and the counterrotation principle does not

necessarily hold for the second histidine. However, since the V/λ value is quite high, indicating a small angle between the two histidine planes (comparison with cyt b_5: 26^o, flavocyt b_2: 13-18^o), the second histidine is expected to be in region 1 rather than in region 2.

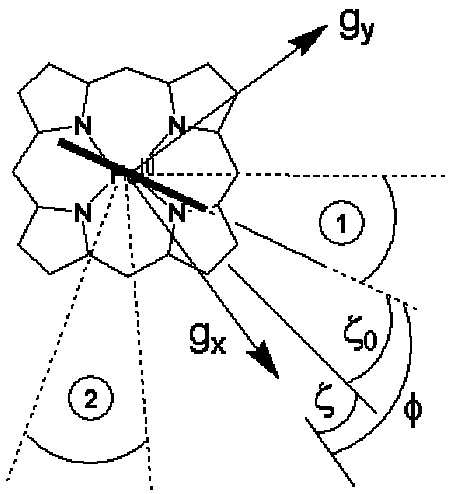

Figure S6: schematic drawing of the orientation of the heme planes based on the EPR data

c) last step in the pulsed EPR analysis

In a last step of the analysis, the contributions of the nearest nitrogens of the axial histidines to the HYSCORE spectra are simulated. Since several of the signals due to these interactions are masked by the contributions of the heme nitrogens, the error on the derived hyperfine and nuclear-quadrupole couplings is larger for the imidazole (Table III) than for the heme nitrogens (Table II). The simulations, taking into account the heme nitrogens and two sets of imidazole nitrogens (related with different tilts of the histidine planes (see above)) are presented in Figure S7 (parameters from Table II and III). Again,

the ambiguity on the rotation direction of the two histidines (related with the angle α in Table III) remains, because both a positive or negative rotation gives similar satisfying fits for the HYSCORE and 3-pulse ESEEM spectra.

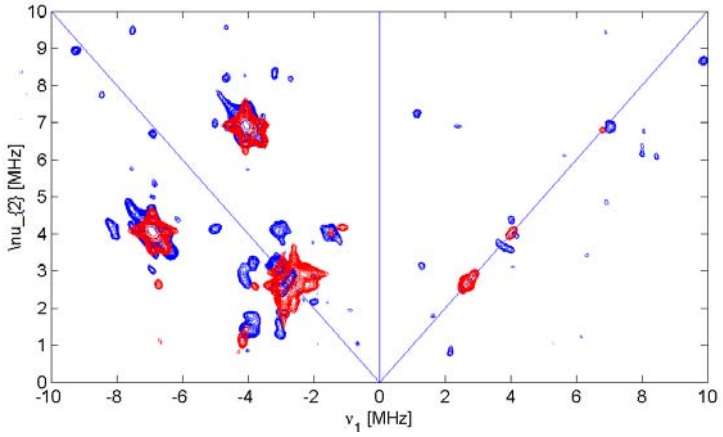

Figure S7 (a): $g=g_z$; simulation of contribution of the porphyrin and histidine nitrogens

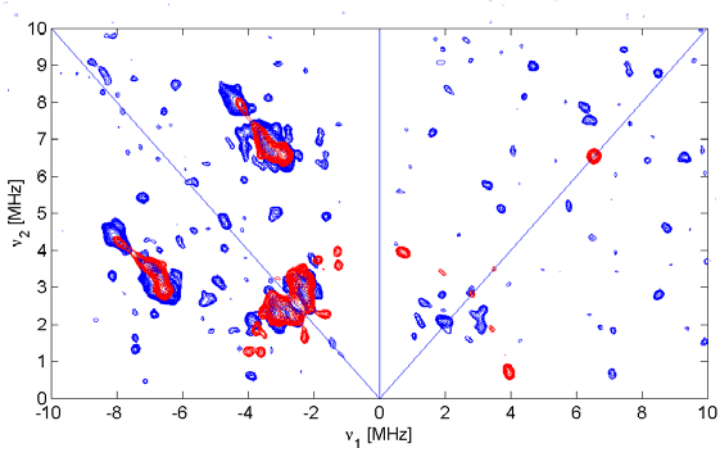

Figure S7 (b): $g=g_y$; simulation of contribution of the porphyrin and histidine nitrogens

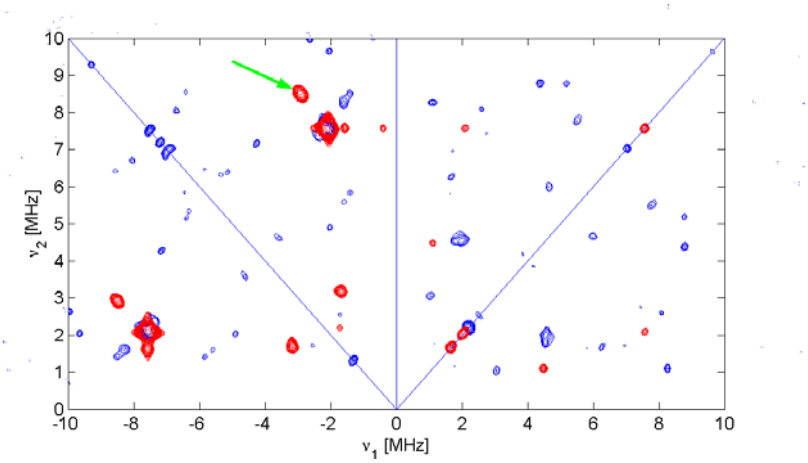

Figure S7 (c): $g=g_x$; simulation of contribution of the porphyrin and histidine nitrogens

Note that in the HYSCORE spectra at $g=g_x$, the cross-peak type marked by the green arrow ((-2.83,8.48) MHz; Figure S7c) is not observable. Due to the low echo-intensity at this high-field position the signal-to-noise of the 2D HYSCORE spectra was too low to resolve this peak. Note however that in the 3-pulse ESEEM spectrum at this position (Figure S2c) a peak at frequency 8.5 MHz is clearly visible.